Interphasial Viscoelastic Behavior of CNT Reinforced Nanocomposites Studied by Means of the Concept of the Hybrid Viscoelastic Interphase

G. C. Papanicolaou,[1] A. G. Xepapadaki,[1] E. D. Drakopoulos,[1] K. P. Papaefthymiou,[1] D. V. Portan[2]

[1]*Department of Mechanical and Aeronautical Engineering, Composite Materials Group, University of Patras, Patras 26500, Greece*
[2]*Department of Applied Chemistry and Materials Science, University Politehnica, Spl. Independentei 313 1, Bucharest, Romania*

Received 27 January 2011; accepted 16 June 2011
DOI 10.1002/app.35202
Published online 20 October 2011 in Wiley Online Library (wileyonlinelibrary.com).

ABSTRACT: In this study the effect of carbon nanotubes content as well as of the tensile stress level applied upon the linear viscoelastic creep response of carbon nanotube polymer nanocomposites was investigated. Experimental findings were modeled by means of the newly developed hybrid viscoelastic interphase model, which constitutes an extension of the previously developed hybrid interphase model. According to this model, the viscoelastic interphase thickness has not of constant value but is dependent upon the property considered at the time as well as on the creep time. In addition, the parameter of imperfect bonding is introduced through the degree of adhesion. Experimental findings combined with analytical results gave a better understanding of the viscoelastic response of epoxy resin carbon nanotubes nanocomposites.
 J Appl Polym Sci 124: 1578–1588, 2012

Key words: nanocomposites; creep; interfaces; viscoelastic hybrid interphase; carbon nanotubes

INTRODUCTION

Nanocomposites are a fairly new category of composite materials, which have attracted extended research activity. Nanoparticles exhibit novel properties that are significantly different than those of the bulk material. Some of these properties are related to large fraction of surface area (several hundreds of square meters per gram[1]), large surface energy, spatial confinement, and reduced imperfections. Thus, only a small amount of nanofillers can significantly change the profile of thermal, electrical, and elastic properties without large increase in the composite's weight. Especially during the last decade, carbon nanotubes have attracted a wide research activity due to their unique behavior. However, carbon nanotubes have first been reported in 1952 by Rykov et al.[2] This discovery passed rather unnoticed and no further investigation took place. After an extended research by Iijima in 1991[3] carbon nanotubes became a new promising material for Nanotechnology. Their excellent mechanical, physical, and other properties,[4–11] such as extremely high elastic modulus and strength, have attracted the researchers' interest, making them a potentially ideal reinforcing material, especially in polymer matrix composites. However, the main difficulty in the manufacturing procedure of nanocomposites is related to the inclusion's strong tendency to agglomerate, which impairs their performance. For this reason, various physical-mechanical (ultrasonication, high speed shearing, etc) or chemical processes (surface modification of nanotubes, or applying in highly acid environment) are used, to improve the degree of dispersion of the nanofillers in the polymer matrix. A critical factor for the behavior of nanocomposites is also the matrix-reinforcement interphasial properties. The interphase is a third phase developed at the close vicinity of the fiber due to the presence micro-cracks, stress concentrations[12–14] residual stresses etc, having properties that are strongly affected by the presence of the reinforcement as well as the imperfect bonding between the two constituent materials. This is the so-called structural interphase,[15] which is formatted spontaneously during the manufacturing of the composite, can be optically observed and should not be confused with the hybrid interphase concept. More precisely, by the term "hybrid interphase," it is meant the interphase material having a volume fraction, which represents the percentage of the bulk matrix surrounding the reinforcement in which a specific

Correspondence to: G. C. Papanicolaou (gpapan@mech.upatras.gr).

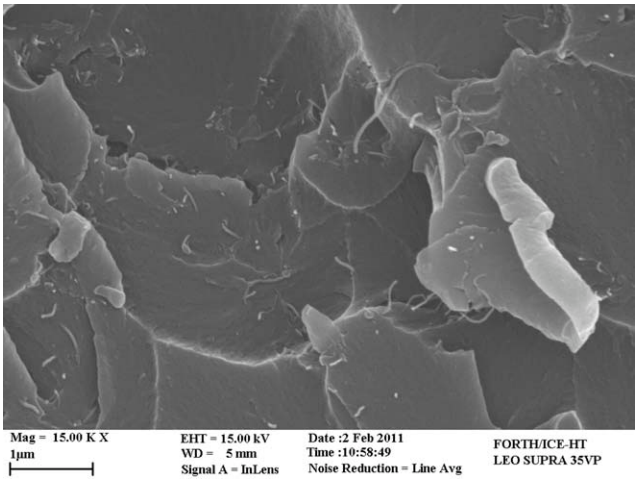

Figure 1 SEM photomicrograph of Epoxy nanocomposite reinforced with 0.3% w_f MWCNT's illustrating good dispersion conditions.

matrix property is strongly affected by the existence of the reinforcement, while the hybrid interphase thickness represents the maximum radial distance from the inclusion boundary in which this property varies. This shows that the interphase is not simply a geometrical concept, dependent only on the volumetric composition of the composite, but it is mainly a property-dependent concept.[16] Recent investigation has proved the validity of the above speculation.[17] For the reasons discussed above, the interphase is a possible place of failure initiation and, consequently, it is important that interphasial phenomena are thoroughly investigated. Although interphasial phenomena between filler and matrix have been extensively investigated and modeled by various researchers,[17–21] only a few works have been concerned on the viscoelastic behavior of the interphase.[22–24] However, the viscoelastic response of structures should be of critical importance especially when they are designed for long-term durability. In this study, the time dependent viscoelastic response of the hybrid interphase was modeled. The effect of the degree of adhesion between the two constituent phases of the composite as well as the effect of creep time upon the degree of degradation of a property and the change in the extent of the interphase thickness were investigated.

EXPERIMENTAL

A diglycidyl ether bisphenol-A (DGEBA)-based (Sigma-Aldrich® 31185 D.E.R.™ 332) was used as epoxy matrix reinforced with Nanothinx S.A.© NTX1 MWNT's. The curing agent was based on TETA (triethylene tetramine; Sigma-Aldrich® 132098). A high-speed shearing method at controlled conditions of pressure, temperature, and speed was used to disperse the nanotubes in the resin. A high-speed dissolver type Dispermat AE, VMA Getzmann GmbH was used for this reason. The quality of dispersion achieved was evaluated by means of SEM fractography. Two extreme conditions of good dispersion and bad quality of dispersion achieved can be observed in Figures 1 and 2, respectively. After several preliminary tests, the process was finally optimized as follows: 2 h mixing the resin with nanotubes in vacuum at 2300 rpm and 50°C. Next, the hardener was added at a ratio of 14 P.H.R. (parts per hundred parts of resin) while mixing procedure was continued. Finally, the mixture was put into special molds and was cured at 80°C for 24 h. After postcuring for 24 h at room temperature, specimens were cut from plates in the desired dimensions with a steel band saw. Each specimen was polished with two types of sand paper to eliminate local surface cracks and surface material heterogeneities.

A series of three point bending tests was performed for various filler weight fractions (w_f = 0, 0.3, 0.7, 1, 2, and 3%) to define the matrix flexural strength, and to statically characterize the nanocomposite. All tests were performed at an INSTRON 4301 universal testing machine. A displacement rate of 1 mm/min was applied in all three-point bending tests. Specimens had dimensions 100 × 12.8 × 2.2 mm^3 (±0.2 mm) and the span between the grips was fixed at 63 mm, according to ASTM D790-99 standard. The results of the flexural moduli, strength, and failure strain presented below represent the mean values from at least three tests at each condition considered.

Tensile creep tests were performed at the linearly viscoelastic region for various fiber loadings [0, 0.3, 1, 2, and 3 w_f (%) MWNT's] and stress levels (σ = 5, 10, and 15% of the matrix strength). The dimensions

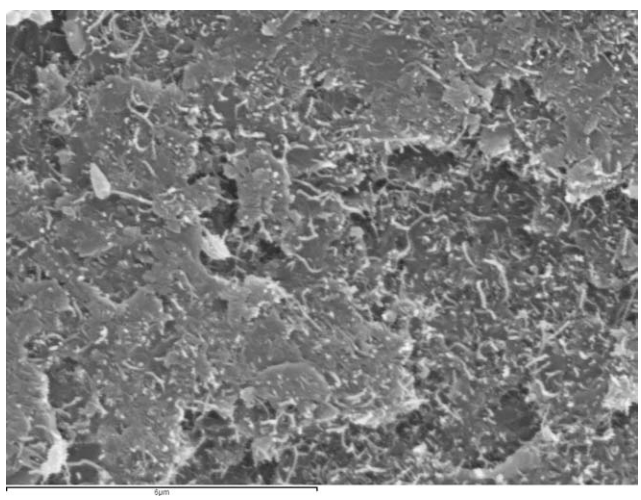

Figure 2 SEM photomicrograph of Epoxy nanocomposite reinforced with 0.3% w_f MWCNT's illustrating poor quality of dispersion conditions.

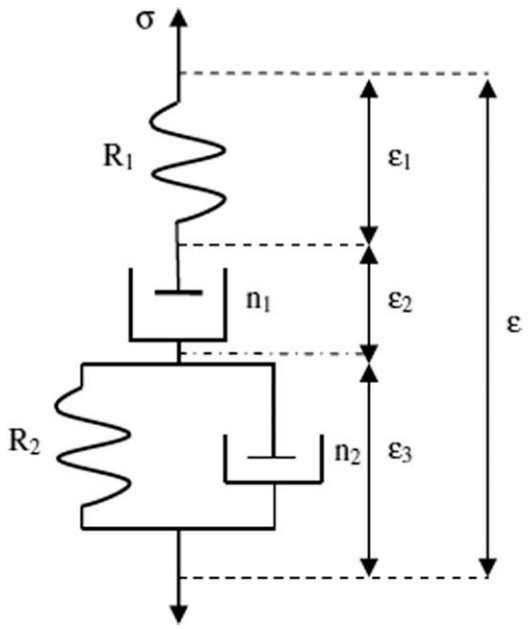

Figure 3 Four parameter model.

of the creep test specimens were 165 × 20 × 3 mm^3. Each test involved a 4 h tensile loading followed by a 3 h recovery. All tests were executed at room temperature (20°C), at an arm lever creep test machine with a ratio of load ranging from 1 : 1 to 1 : 5. The vertical displacement was measured by an LVDT sensor of RDP Electronic. An A/D converter of National Instruments Co was used for the data acquisition, which was automatically recorded with the corresponding time using LabView® v.60 software. At least three creep tests were performed for each condition to ensure reproducibility.

Background

In this investigation linear viscoelastic behavior was considered for the interphase material. For reasons of simplicity, to model this behavior the four-element model was applied.

The four element model

The ideal linearly elastic solid can be modeled by a spring and however, a Newtonian fluid's perfectly viscous behavior can be represented by a dashpot. A material's viscoelastic response incorporates characteristics of both an elastic solid and a viscous fluid. There have been developed various constitutive models to model its behavior and are a combination of the above ideal elements. A simple model is the four-parameter model (Fig. 3), which consists of a Kelvin and a Maxwell model in a row can be applied assuming that the presuppositions of linear viscoelastic behavior were fulfilled.[25,26] The relationship between σ and ε can be given by the constitutive equation:

$$\sigma + \left(\frac{n_1}{R_1} + \frac{n_1}{R_2} + \frac{n_2}{R_2}\right)\dot{\sigma} + \frac{n_1 n_2}{R_1 R_2}\ddot{\sigma} = n_1\dot{\varepsilon} + \frac{n_1 n_2}{R_2}\ddot{\varepsilon} \quad (1)$$

where R_1, R_2 exhibit instantaneous elasticity and recovery and can be interpreted as a Young's modulus. The parameters n_1, n_2 are called coefficients of viscosity. The creep compliance, $C(t)$ is a time dependent function relating the creep strain developed in the material, $\varepsilon(t)$, which is the response to the constant creep load applied to it, σ_0, under constant environmental conditions.

$$\varepsilon(t) = C(t)\sigma_0 \quad (2)$$

Thus, the creep compliance and strain of the four-element model derived from eqs. (1) and (2) can be found as follows:

$$C(t) = \frac{1}{R_1} + \frac{1}{n_1}t + \frac{1}{R_2}\left(1 - e^{\frac{-R_2 t}{n_2}}\right) \quad (3)$$

$$\varepsilon(t) = \frac{\sigma_0}{R_1} + \frac{\sigma_0}{n_1}t + \frac{\sigma_0}{R_2}\left(1 - e^{\frac{-R_2 t}{n_2}}\right) \quad (4)$$

If the creep stress is removed at time $t = t_1$, then the recovery behavior of the four-element model can be obtained by eq. (5):

$$\varepsilon(t) = \frac{\sigma_0}{n_1}t_1 + \frac{\sigma_0}{R_2}\cdot\left(1 - e^{-\frac{R_2 t_1}{n_2}}\right)\cdot e^{-\frac{R_2(t-t_1)}{n_2}} \quad (5)$$

Also the creep rate, $\dot{\varepsilon}$ is given by

$$\dot{\varepsilon}(t) = \frac{\sigma_0}{n_1} + \frac{\sigma_0}{n_2}e^{-\frac{R_2 t}{n_2}} \quad (6)$$

The parameters R_1, n_1, R_2, and n_2 represent intrinsic characteristics of a viscoelastic material. The spring element R_1 represents the linearly elastic component of the stiffness and can be obtained from the instantaneous strain, ε_1, when a creep load is applied. The dashpot constant n_1, is connected with the viscoelastic, nonreversible component of deformation and is obtained from the slope of the creep curve in the steady state region, $\underline{\varepsilon_2}$. The stiffness constant R_2 is connected with the reversible component of the viscoelastic deformation and is obtained from the maximum retarded deformation, ε_3. Finally, the dashpot coefficient n_2, which reflects the viscous reversible deformation in the region where the retarded elasticity dominates, can be quantified with substitution in eq. (6) for a point of the curve.

Theoretical approach of the viscoelastic hybrid interphase model

The viscoelastic modeling of the hybrid interphase behavior requires various assumptions regarding the

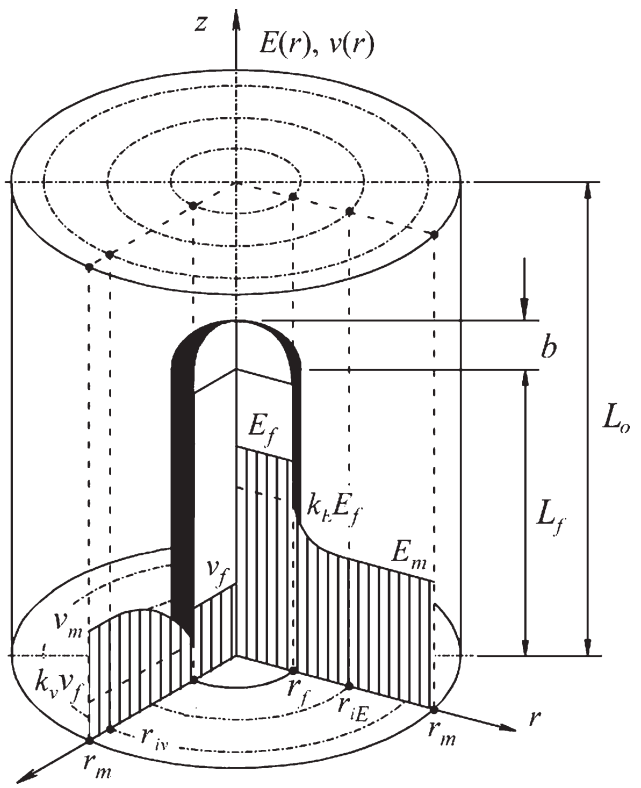

Figure 4 RVE incorporating the concept of hybrid interphase.

elastic response, geometry, etc. Some typical geometric assumptions are that fibers are perfectly cylindrical, unidirectional, continuous, and uniformly spaced. Some typical assumptions regarding the material properties are: (i) the fibers behave in a linearly elastic manner whereas the matrix is linearly viscoelastic; (ii) the fibers are transversely isotropic; (iii) the global composite behavior can be modeled by a representative volume element (RVE). Assuming a periodic configuration of fibers, micromechanical analysis requires the selection of a proper RVE, which must contain a single fiber, adjoining interphase and bulk matrix. Figure 4 illustrates the RVE of the problem considered and the material properties (elastic modulus, E, and Poisson's ratio, ν, etc) variation within the interphase region. The bounding surfaces of the RVE are subjected to constraints that are consistent with the structural periodicity and the far field loading. Since the effect of fiber tip radius of curvature, b, on the volumetric composition is negligible, material inhomogeneities, and thus the composite cylinder in the RVE considered with length L_0 can be described in terms of a two-dimensional cylindrical coordinate system (r, z). In the RVE considered, a solid circular cylinder of radius r_f and half-length L_f simulates the fiber, the outer radius of the matrix r_m is identical to that of the RVE, and indices f, m indicate fiber and matrix phases, respectively. Finally, as it will be shown below, the property value at the fiber-matrix boundary is $k_E E_f$ and $k_\nu \nu_f$, where k represents the adhesion efficiency coefficient while r_{iE} and $r_{i\nu}$ represent the outer boundary of the hybrid interphase corresponding to the stiffness, E, and Poisson's ratio, ν, respectively.

The hybrid interphase is not a theoretical assumption and its existence has been proved experimentally.[17] The concept of the hybrid interphase is based on two assumptions. The first one accepts a nonhomogeneous interphase whose material properties depend on the respective properties of a homogeneous fiber and matrix, and thickness depending on volumetric composition of composite.[27] The second assumption introduces imperfect adhesion between fiber and matrix materials [eq. (11)] by proper definition of material properties.

Assuming perfect bonding between the fiber-matrix interface, there is no relative displacement between fiber and matrix at the interface, and that the properties along the hybrid interphase reach the respective values of the matrix in a smooth way, we derive to the following conclusions

$$E_i(r = r_{iE}, t) = E_m(t) \tag{7}$$

$$\left.\frac{\partial E_i(r = r_{iE}, t)}{\partial r}\right|_{t=t_0} = 0 \tag{8}$$

$$E_i(r = r_f, t) = E_f \tag{9}$$

$$\left.\frac{\partial E_i(r_f^-)}{\partial r}\right|_{t=t_0} \neq \left.\frac{\partial E_i(r_f^+)}{\partial r}\right|_{t=t_0} \tag{10}$$

where indices f, i, m denote fiber, interphase, and matrix, respectively, r_{iE} represents the outer boundary of the hybrid interphase based on the stiffness, while the superscripts, "$-$" and "$+$" represent a position infinitely close before and after the fiber-matrix boundary

It is obvious that perfect bonding between fiber and matrix does not exist in reality due to the existence of flaws and roughness at the fiber surface, and other physical and mechanical interactions. This imperfection is described by the adhesion efficiency coefficient

$$k_E(t) = \frac{E_i(r_f^+, t)}{E_f} \tag{11}$$

which represents the discontinuity of the properties that occur at the fiber-matrix interface. The coefficient k_E describes equivalently the efficiency of bonding for the modulus of elasticity defined by the eq. (11). This equation imposes a jump on material properties and can take values $0 \leq k_E \leq 1$. The limit value $k_E = 1$ describes a compliant interphase with perfect adhesion conditions, in which full stress transfer occurs. When its value is zero, no stress

transfer occurs because of any adhesion. In real conditions of imperfect adhesion, where $0 < k_E < 1$, only a segment of the stresses are transferred from the matrix to the fiber through the interphase. The above account for any material property such as Poisson's ratio, ν, thermal expansion coefficient, α, etc. With regard to eq. (11), eq. (9) becomes

$$E_i(r = r_f^+, t) = k_E(t)E_f \tag{12}$$

Obviously, for a given value of time $t = t_0$, the gradient of E_i is inversely proportional to the interphase thickness. Also, if an exponential variation of properties is assumed, or in other words the gradient of a value with respect to the distance from the fiber at the radial direction being proportional to its value we obtain:

$$\left.\frac{\partial E_i(r,t)}{\partial r}\right|_{t=t_0} = -c_E \cdot (E_i(r, t = t_0) - E_m(t = t_0)), \quad r_f \le r \le r_{iE} \tag{13}$$

where

$$c_E = (t_E)^{-1}, \quad t_E = r_{\mathrm{iE}} - r_f \tag{14}$$

One of the factors that affect the interphase thickness is the adhesion efficiency coefficient, k_E. The lower values the adhesion efficiency coefficient takes, the more inefficient is the connection between the fiber and the matrix macromolecules. As the molecules of the matrix are improperly jointed to the fiber surface, the interphase thickness increases. Moreover, the mechanical properties at the transverse direction are dominated by the matrix and consequently the portion of the matrix that is affected by the presence of the fiber, or in other words the interphase extent. On the contrary, the material's properties at the longitudinal direction are principally affected by the fiber. As a result, the interphase thickness should be proportional to the anisotropy coefficients of the material, S_E, and S_ν.[28,29] Also, the value of a property at the longitudinal direction is proportional to the filler volume fraction and to the fiber radius. To sum up, the interphase thickness can be given by the equation below:

$$t_E = S_E \cdot r_f \cdot \frac{1 - k_E}{k_E} \tag{15}$$

where

$$S_E = \frac{E_T}{E_L} \tag{16}$$

where the E stands for the respective property of the bulk composite (Elastic modulus) and the indices T and L denote the value of a property at the transverse and the longitudinal direction, respectively. Assuming perfect bonding between fiber and matrix, fibers periodically distributed, linear and parallel to each other and linearly elastic response, we obtain the rule of mixtures parallel to the axis of the fibers and normal to them

$$E_l = E_f\upsilon_f + E_m(1 - \upsilon_f)\,, \qquad E_t = \frac{E_f E_m}{E_f(1 - \upsilon_f) + E_m\upsilon_f} \tag{17}$$

Applying eqs. (14–16) into eq. (13) we obtain

$$\left.\frac{\partial E_i(r,t)}{\partial r}\right|_{t=t_0} = -\frac{E_l}{E_t}\frac{k_E}{r_f(1 - k_E)}(E_i(r,t) - E_m(t)) \tag{18}$$

Solving the above equations with respect to the boundary conditions eqs. (8), (9), and (11) we obtain the variation of the elastic properties of the interphase as a function distance from the fiber surface and the adhesion efficiency coefficient. Thus, as shown in a previous publication,[30] the degradation of the elastic properties within the hybrid interphase region is given by:

$$E_i(r,t) = E_m(t) + \left(k_E E_f - E_m(t)\right) \exp\left\{-\frac{k_E}{1 - k_E}\frac{E_L}{E_T}\frac{r - r_f}{r_f}\right\}, \quad r_f \le r \le r_{iE} \tag{19}$$

where E_f is the fiber's (nanotube) modulus; E_i is the interphase modulus; $E_m(t)$ is the matrix modulus as a function of creep time; E_L and E_T are the macroscopic elasticity moduli of the bulk composite along the longitudinal and the transverse direction, respectively; k_E is the fiber-matrix adhesion efficiency coefficient with respect to the Young's Modulus.

When subjected to creep, the matrix modulus, E_m, is inverse to the creep compliance, $C(t)$ and can be determined either experimentally or by a theoretical model. The application of the four-element model upon the creep curves gives:

$$Em(t) = (C(t))^{-1} = \left(\frac{1}{R_1} + \frac{1}{\eta_1}t + \frac{1}{R_2}\cdot\left(1 - e^{-\frac{R_2 t}{\eta_2}}\right)\right)^{-1} \tag{20}$$

RESULTS AND DISCUSSION

Static characterization of nanocomposites

The effect of CNT's weight fraction upon the nanocomposite's flexural modulus, strength, and failure strain is presented in Figure 5(a,c). A significant

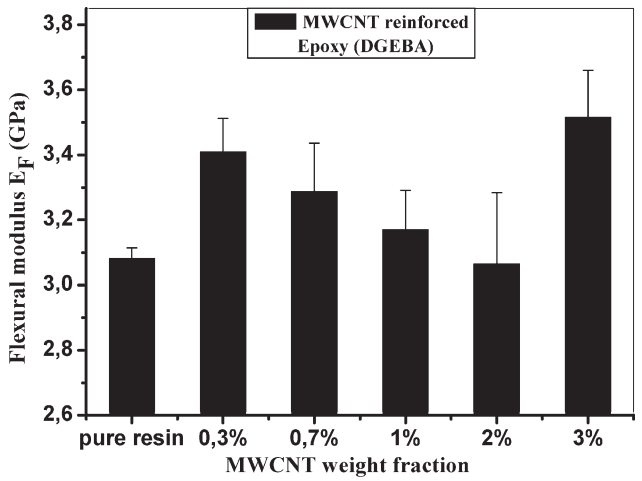

(a)

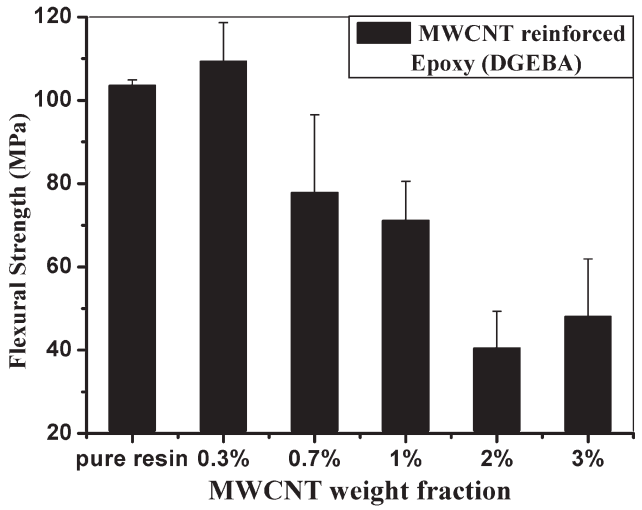

(b)

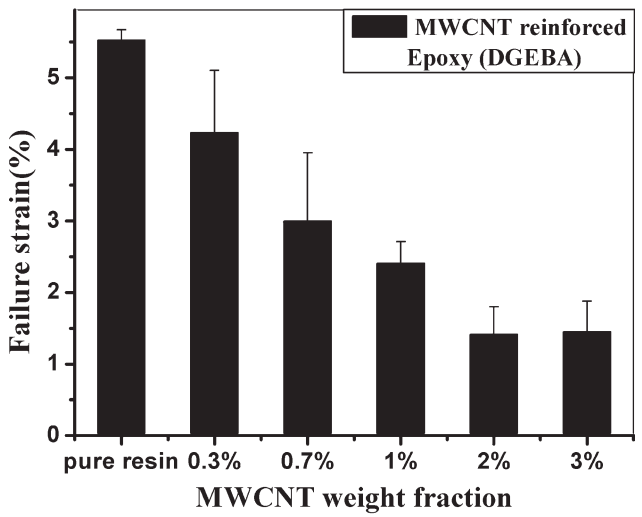

(c)

Figure 5 (a) Flexural modulus, (b) Ultimate flexural strength, and (c) Failure strain of Epoxy nanocomposite as a function of weight fraction in MWCNT's.

increase of 10.6 and 14.03% of the Young's modulus was measured for 0.3% w_f and 3% w_f, respectively. In addition, as shown in Figure 5(b,c) general reduction in both flexural strength and failure strain was observed. The higher the CNT weight fraction is, the more brittle the nanocomposite becomes. This type of mechanical behavior can be attributed to more than one reason. Among the principal mechanisms that affect the behavior of the composite are the adhesion and agglomeration, two competing phenomena that have converse effect on the material behavior. Concerning the modulus of elasticity [Fig. 5(a)], at low weight fractions, a macroscopic increase of the modulus is being observed due to low agglomeration of filler particles. As the content in nanotubes increases, so does the degree of agglomeration which results in voids, microcracks, deficient wetting, etc. These phenomena become more intense and dominate upon the increasing of stiffness that is caused by the addition nanotubes and the modulus of the composite material reaches a minimum at $w_f = 2\%$. However, after a further increase in the MWCNT's weight fraction, an increase in the modulus of the material is observed, due to their outstandingly high stiffness combined with the effect various antagonistic phenomena. For a given weight fraction, the number of filler particles found in a unit volume of a nanocomposite is several orders of magnitude higher than the respective number of fillers in the case of a micro-composite. So, the critical weight fraction for the clustering to occur is expected to be significantly lower. As a result, in a nanocomposite with a high filler volume fraction ($\sim$ 3%), one may deduce two possible microstructures in addition to that where particles are randomly dispersed. In the first case, the resin is completely entrapped within the filler aggregates or clusters, with fibers touching each other. In the second type of microstructure, the composite contains a mix of regions with randomly dispersed particles and regions of resin entrapped within fiber clusters. In principal, such composites would consist of regions with randomly dispersed fillers, but with each region containing a different volume fraction.[31]

Regarding the flexural strength [Fig. 5(b)], the reinforcing ability of MWCNT's is undermined by the effect of agglomeration. For low weight fractions, where the agglomerates are smaller, resulting in higher surface area, loads can be transferred to the nanotubes, resulting in a considerable increase of the ultimate strength. Although, increasing the filler's weight fraction the degree of agglomeration causes a more brittle behavior for the following reasons. Reduced surface area results in inefficient load transfer from matrix to nanotubes, while agglomeration, voids, microcracks, and other discontinuities, constitute points of local stress concentrations. The

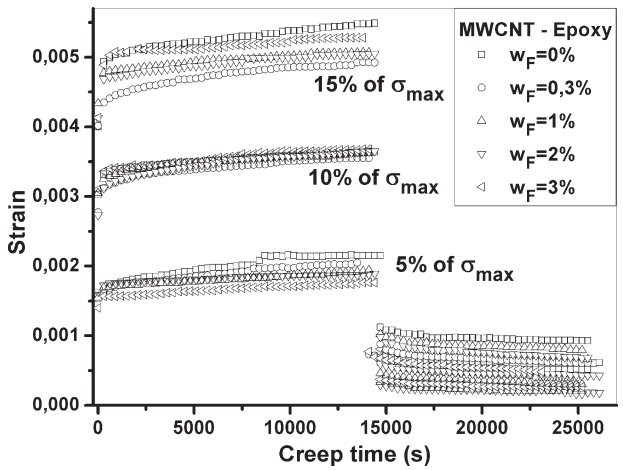

Figure 6 Effect of filler's weight fraction upon the creep behavior of MWCNT-Epoxy nanocomposites for different creep load levels.

degradation of the material's failure strain [Fig. 5(c)] is also attributed to analogous phenomena. However, besides these two factors, many others should be taken into account to understand what lies behind the above behavior.

Creep behavior of nanocomposites

Creep curves of nanocomposites for different stress levels and different fiber loadings are illustrated in Figure 6. Each group represents a different constant load applied to the material. The magnitude of loadings has been opted to be relatively low compared to the matrix strength so as to assure a linearly viscoelastic response at room temperature. The respective curves of the creep compliance of the tested specimens are also shown in Figure 7. A loading of 5% of σ_{max} an important fall of 27.32% on the basis of pure resin was measured for $w_f = 1\%$ at a creep time when steady state creep was achieved ($t = 12{,}500$ s). For higher loadings the amplitude of divergence was found to decrease as the creep stress increased. The creep compliance measured for stress levels of 10% of σ_{max} and 15% of σ_{max} was lower by 9.32 for 1% w_f and 3.98 for 2% w_f, respectively. From the above behavior, it can be inferred that when subjected to higher loadings, the filler has reduced capacity to increase the material's stiffness. Under increased stress or strain levels the degree of adhesion between the matrix and the nanotubes is thought to deteriorate. Thus, a mediocre quality of bonding leads to inefficient load transfer from the matrix to the MWCNT's, which are meant to stiffen the material.

When being in the linear viscoelastic region the Boltzmann superposition principle dictates that for a given time there exists a linear relation between applied creep stress and creep strain.[25] This line is referred as isochronous curve and its slope is defined as creep modulus, E_{creep}. The variation of the material's creep modulus as a function of the w_f in MWCNT's for various creep times is presented in Figure 8. It can be observed that the creep modulus

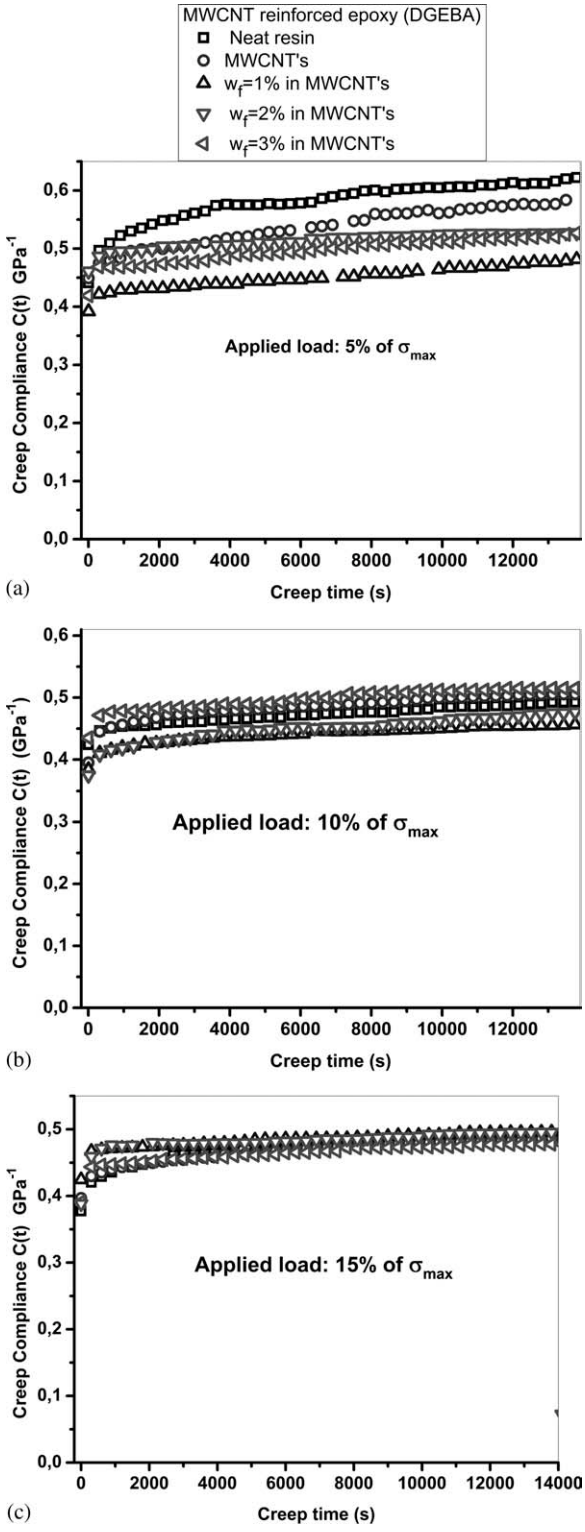

Figure 7 Creep compliance of nanocomposites for different weight fractions in MWCNT's-Applied load: (a) 5%, (b) 10%, and (c) 15% of matrix' ultimate strength.

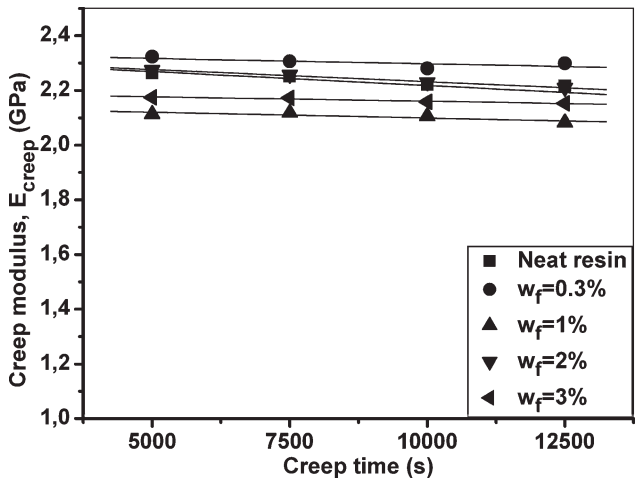

Figure 8 Creep modulus of MWCNT-Epoxy nanocomposite as a function of time for various filler weight fractions.

is weakly dependent on the filler content. However, it reaches its maximum value for 0.3% w_f and it follows the same trend as the Young's modulus. In addition, the magnitude of degradation of creep modulus found to be greater for the unfilled resin than the composite.

Viscoelastic modeling

Four element model

Since the requirements of linear viscoelasticity were fulfilled for the whole range of applied loadings and creep times, the application of the four-element model is considered valid. The variation of R_1 as a function of w_f in MWCNT's for different applied loads, normalized on the basis of the respective value of the pure resin is illustrated in Figure 9(a). A similar behavior to the Elastic modulus is observed, which is rather expected, since the parameter R_1 represents the instantaneous reverse elastic component of the materials' deformation. The phenomena that dominate this type of behavior are being discussed above. Moreover, a difference in the values of R_1 is being measured for the various applied loads. R_1 takes higher values, compared to pure resin, for lower levels of creep stress. At 1% w_f

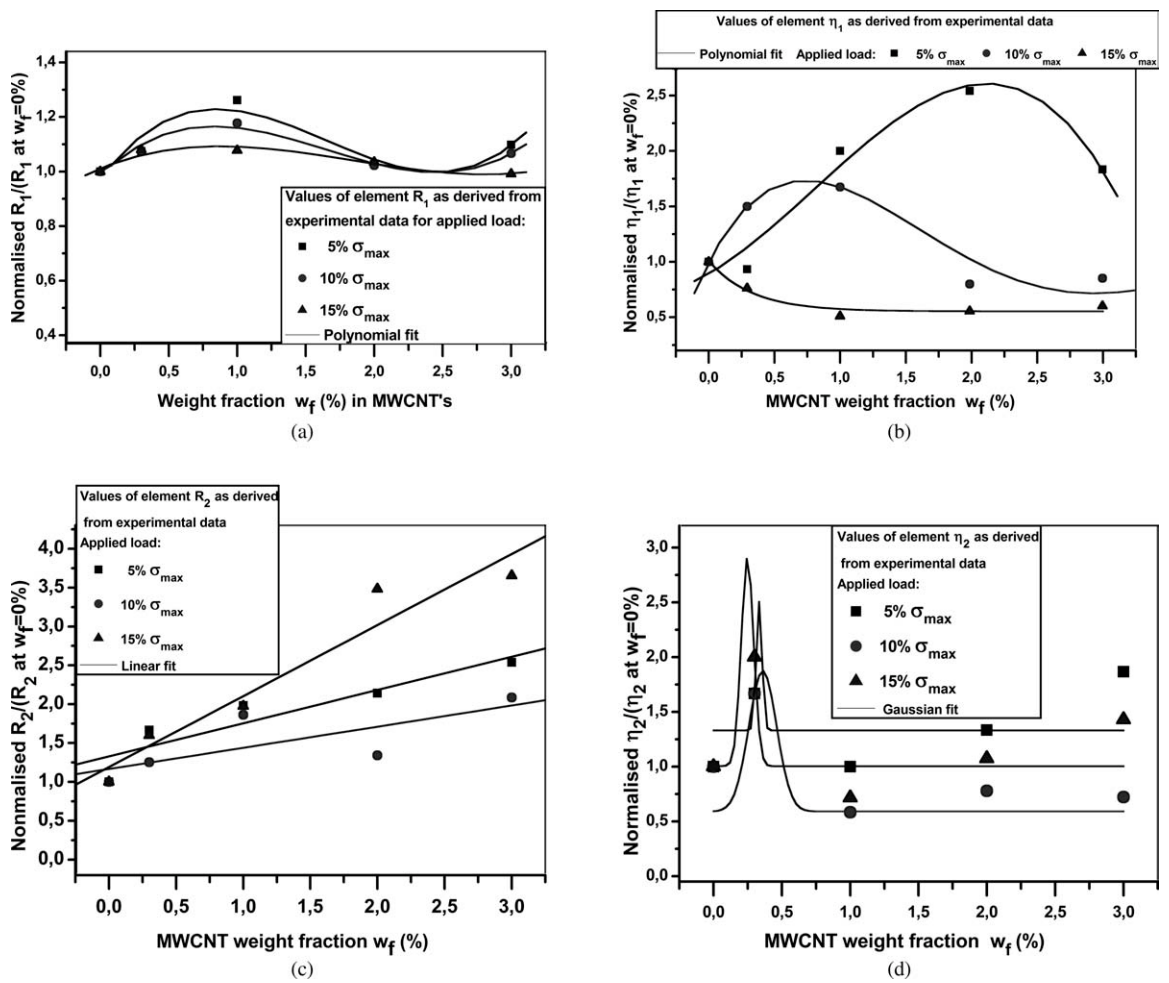

Figure 9 Normalized (a) instantaneous elasticity, R_1, (b) viscosity, n_1, (c) retarded elasticity, R_2, and (d) viscosity, n_2, of epoxy nanocomposite, as a function of weight fraction in MWCNT's for various levels of creep load.

an increase of 26.16% is measured for a load of 5% of σ_{max}. The raise measured for stress levels of 10% of σ_{max} and 15% of σ_{max} was 17.77 and 8.01%, respectively. This behavior, as mentioned above, is in relation to the interphasial strength between the nanotubes and the matrix. For higher loads, there is higher possibility of local failure of the interphasial bond, which hinders the stress transfer from the matrix to the fiber.

The variation of n_1 based on neat resin as a function of filler content and for different creep stress levels is illustrated at Figure 9(b). For low stress levels, the parameter n_1 increases almost proportionally with filler content and for 2% w_f reaches a maximum factor of 2.54. This behavior denotes a less viscoelastic material that exhibits lower creep rate at steady state. For higher weight fractions the value of n_1 slightly falls, which implies that the stiffening ability of the nanotubes has been saturated due to the presence of filler aggregates, clusters, deficient adhesion, and other parameters that affect the material's microstructure. For intermediate loadings (10% of σ_{max}) the same behavior is exhibited, although, the fall in the value of n_1 is of higher magnitude and is observed at lower content of MWNT's. Finally, for stress levels of 15% of σ_{max}, a slight decrease in the value of n_1 is noticed as a result of the effect of the presence impurities on the interphasial bonding and the stress transfer between the two constituent phases.

The element R_2 represents the material's retarded elastic reverse deformation. Its variation versus filler's weight fraction for different values of applied creep load is presented in Figure 9(c). A significant raise in R_2 is observed, compared to pure resin, with the increase of filler content, especially for higher stress levels. At $w_f = 3\%$ an increase by a factor of 3.65 is measured for a load of 15% of σ_{max}. The increase in R_2 at lower loads was calculated as 2.09 and 2.54 times higher for loads of 10 and 5% of σ_{max}, respectively. This behavior can be explained as follows: with the addition of nanotubes, the material tends to exhibit its elastic rather than its viscous nature, which leads to an increase in R_2. Apparently, this behavior becomes more evident for higher weight fractions in CNT's. Moreover, the fact that this behavior is more evident for higher creep loads indicates an increase of the effect of the reinforcement upon the parameter R_2.

The dashpot element of the Kelvin-Voigt component, n_2, represents the viscosity related with the material's retarded viscoelastic reverse deformation. The variation of n_2 as a function of filler content based on neat resin and for different creep stress levels is presented in Figure 9 days. The parameter n_2 was found to increase as a function of filler content up to a maximum value of 98.2% with respect to the neat resin. Nanofillers impose restrictions to the relative displacement of polymer chains, which is responsible for a macroscopic increase in the material's viscosity. However, at high CNT's weight fractions the filler-matrix surface area is reduced due to the effect agglomeration and, consequently, the reversible viscosity, n_2, recedes.

TABLE I
Multiwalled Carbon Nanotubes' and Epoxy Resin's Properties

Fiber		Matrix			
E_f (GPa)	r_f (nm)	R_1 (GPa)	n_1 (Pa s)	R_2 (GPa)	n_2 (Pa s)
704	12.5	2.65	4.33×10^{14}	1.06	1.93×10^{13}

Viscoelastic hybrid interphase model

The interphasial elastic and viscoelastic properties follow a specific exponential law of variation, depending on the degree of adhesion between fiber and matrix. The four-element Maxwell-Kelvin model is incorporated to model matrix the compliance against a constant creep load. A series of parametric studies is carried out to examine the effect of adhesion conditions and creep time on the variation of the interphase modulus as well as the hybrid interphase thickness. The properties of the MWCNT's (as provided by the manufacturer) and the matrix (experimentally determined in the linearly viscoelastic region) applied for the proposed model can be found in Table I. The model of viscoelastic hybrid interphase was applied for several values of creep time and adhesion efficiency coefficient. The results concerning the interphase modulus are illustrated in Figure 10. It can be observed that as we move far from the fiber the viscoelastic nature of the interphase becomes more apparent. This is interpreted as a stronger dependence of the interphase modulus on time and stems from the fact that the viscoelastic behavior of the interphase matrix-dominated. In addition, the interphase thickness versus creep time was predicted based on the arbitrary assumption that the interphase region lies in the region that extends from the fiber's surface up to the point where the deflection between the interphase modulus and the matrix modulus is $\sim 1\%$. The variation of interphase thickness as a function of creep time is depicted in Figure 11(a,b), assuming conditions of poor quality of adhesion ($k_E = 0.20$) and perfect adhesion ($k_E = 0.99$), respectively. The interphase thickness is found to exhibit a tendency to expand with time, following an exponential law of variation. Assuming a periodic hexagonal array of inclusions, for volume fractions $\upsilon_f = 0.5\%$ or higher the interphases round neighboring nanotubes overlap, which

results to a transformed matrix with distinct properties from the pure resin. Moreover, the interphase thickness as well as the magnitude of its increase versus time is found to be a strong function of the efficiency of the CNT-matrix bonding. This behavior is attributed to the effect of degree of adhesion upon the load transfer from the matrix to the fiber and the efficient transfer of the fiber's properties to the composite through the interphase. Thus, a poor degree of adhesion hinders the transfer of the fiber's properties through the interphase. Consequently, for less efficient bonding between the two constituent phases, the mechanical behavior of the interphase is dominated by the matrix at a higher extent, and thus the viscoelastic response of the interphase and variation of its thickness with time will be more intense.

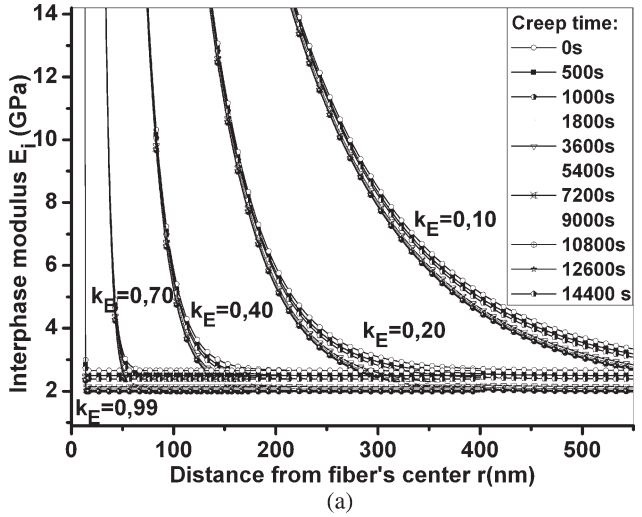

(a)

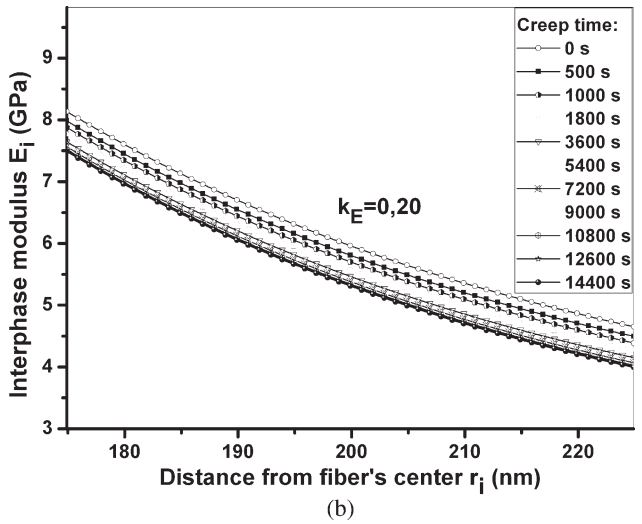

(b)

Figure 10 Prediction of viscoelastic hybrid interphase modulus as a function of the distance from the nanotube, for (a) various values of adhesion efficiency coefficient, k_E and (b) adhesion efficiency coefficient, $k_E = 0.20$ in MWCNT-Epoxy nanocomposite. The dots represent the theoretical values, while the continuous line the fitting curves.

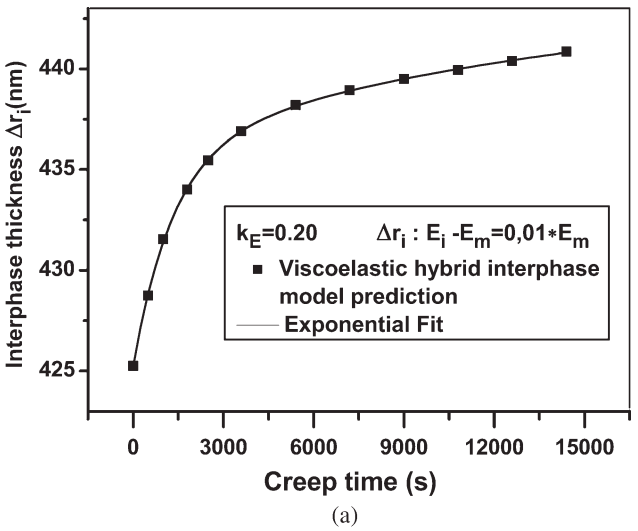

(a)

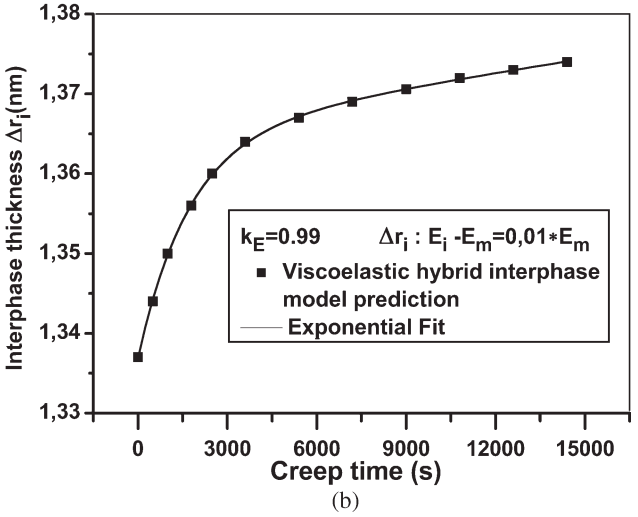

(b)

Figure 11 Prediction of the thickness of the viscoelastic hybrid interphase in MWCNT epoxy nanocomposite, as a function of creep time (a) for poor quality of adhesion ($k_E = 0.20$) and (b) assuming perfect adhesion ($k_E = 0.99$). The dots represent the theoretical values, while the continuous line the fitting curves.

CONCLUSIONS

In this work, the effect of filler content upon the macroscopic mechanical and viscoelastic behavior of MWCNT-Epoxy nanocomposites, through static three point bending tests and creep tests at various stress levels. The material's stiffness reaches a maximum at relatively low filler weight fractions, above which the impact of inclusion on the material's response is weaker. This is attributed primarily to two competing phenomena that have opposite effect on the nanocomposite's response: adhesion and agglomeration. Moreover, the filler's reinforcing ability was found to be stronger for lower creep loads, which implies gradual failure of interfacial bonding as loads increase. From the above it can be inferred that the nanocomposite's manufacturing procedure

should be optimized with emphasis on the dispersion on the nanotubes in the resin, to take advantage of the filler's unique mechanical properties. Given that interfacial phenomena and the interphase region in general are critical for the composite's global response, the viscoelastic behavior of the interphase was modeled by introducing the concept of viscoelastic hybrid interphase. The viscoelastic behavior of the interphase is matrix-dominated and becomes more apparent as we move far from the fiber. Results show a considerable influence of time and a strong impact of the degree of adhesion between the constituent phases on the hybrid interphase properties and extent, which affects the overall viscoelastic response of fiber-reinforced composites.

References

1. Peigney, A.; Laurent, Ch.; Flahaut, E.; Bacsa, R. R.; Rousset, A. Carbon 2001, 39, 507.
2. Rykov, V. T.; Lukyanovich, V. M.; Radushkevich, L. V. Bull Acad Sci USSR Phys Ser 1952, 1, 395.
3. Iijima, S. Nature 1991, 354, 56.
4. Treacy, M. M. J.; Ebbesen, T. W.; Gibson, J. M. Nature 1996, 381, 678.
5. Wong, E. W.; Sheehan, P. E.; Lieber, C. M. Science 1997, 277, 1971.
6. Salvetat, J. P.; Bonard, J. M.; Thomson, N. H.; Kulik, A. J.; Forro, L.; Benoit, W.; Zuppiroli, L. Appl Phys A 1999, 69, 255.
7. Yu, M. F.; Files, B. S.; Arepalli, S.; Ruoff, R. S. Phys Rev Lett 2000, 84, 5552.
8. Robertson, D. H.; Brenner, D. W.; Mintmire, J. W. Phys Rev Lett B 1992, 45, 12592.
9. Yakobson, B. I.; Brabeck, C. J.; Bernholc, J. Phys Rev Lett 1995, 76, 2511.
10. Belytschko, T.; Xiao, S. P.; Schatz, G. C.; Ruoft, R. S. Phys Rev Lett B 2002, 65, 235430.
11. Lu, J. P. Phys Rev Lett 1997, 79, 1297.
12. Cox, H. L. Brit J Appl Phys 1951, 3, 72.
13. Theocaris, P. S.; Papanicolaou, G. C. Fibre Sci Tech 1979, 12, 421.
14. Haque, A.; Ramasetty, A. Compos Struct 2004, 71, 68.
15. Papanicolaou, G. C.; Anifantis, N. K.; Keppas, L. K.; Kosmidou, Th. V. Compos Interf 2007, 14, 131.
16. Papanicolaou, G. C.; Michalopoulou, M. V.; Anifantis, N. K. Compos Sci Technol 2002, 62, 1881.
17. Kim, J. K.; Sham, M. L.; Wu, J. Compos A 2001, 32, 607.
18. Hiemstra, D. L.; Sottos, N. R. J Compos Mater 1993, 27, 1030.
19. Chouchaoui, C. S.; Benzeggah, M. L. Comp Sci Tech 1997, 57, 617.
20. Pompe, G.; Mäder, E. Comp Sci Tech 2000, 60, 2159.
21. Jayaraman, K.; Reifsnider, K. L. Comp Sci Tech 1993, 47, 119.
22. Fisher, F. T.; Brinson, L. C. Comp Sci Tech 2001, 61, 731.
23. Li, J; Weng, G. J Comp 1996, 27B, 589.
24. Wei, P. J.; Huang, Z. P. Int J Sol Struct 2004, 41, 6993.
25. Papanicolaou, G. C.; Xepapadaki, A. G.; Karagounaki, K.; Zaoutsos, S. P. J Appl Polym Sci 2008, 108, 640.
26. Bertilsson, H.; Jansson, J. F. J Appl Polym Sci 1971 1975, 19.
27. Lipatov, Y. S. Physical Chemistry of Filled Polymers (translated from the Russian by R. JMoseley). Int Polym Sci Tech Monog 1977, 2.
28. Jayaraman, K.; Reifsnider, K. L.; Swain, R. E. J Comp Tech Res 1993, 15, 14.
29. Kakavas, P. A.; Anifantis, N. K.; Baxevanakis, K.; Katsareas, D. E.; Papanicolaou, G. C. J Mater Sci 1995, 30, 4541.
30. Papanicolaou, G. C.; Demetrescu, I.; Portan, D. V.; Papaefthymiou K. P. Comp Interf 2011, 13, 23.
31. Wu, W.; Sadeghipour, K.; Boberick, K.; Baran, G. Mater Sci Eng A 2002, 332, 362.